IceRay: An IceCube-centered Radio-Čerenkov GZK Neutrino Detector

P. Allison[a], J. Beatty[b], P. Chen[c], A. Connolly[d], M. DuVernois[a], P. Gorham[a], F. Halzen[e], K. Hanson[e], K. Hoffman[f], A. Karle[e], J. Kelley*[,e], H. Landsman[e], J. Learned[a], C. Miki[a], R. Morse[a], R. Nichol[d], C. Rott[b], L. Ruckman[a], D. Seckel[g], G. Varner[a], D. Williams[h]

[a]*Dept. of Physics and Astronomy, Univ. of Hawaii, Manoa, HI 96822, USA*
[b]*Dept. of Physics, Ohio State University, Columbus, OH 43210, USA*
[c]*Dept. of Physics, National Taiwan Univ., Taipei 106, Taiwan*
[d]*Dept. of Physics & Astronomy, Univ. College London, London WC1E 6BT, UK*
[e]*Dept. of Physics, Univ. of Wisconsin, Madison, WI 53703, USA*
[f]*Dept. of Physics, Univ. of Maryland, College Park, MD 20742, USA*
[g]*Dept. of Physics and Astronomy, Univ. of Delaware, Newark, DE 19716, USA*
[h]*Dept. of Physics and Astronomy, Univ. of Alabama, Tuscaloosa, AL 35487, USA*

Abstract

We discuss design considerations and simulation results for IceRay, a proposed large-scale ultra-high energy (UHE) neutrino detector at the South Pole. The array is designed to detect the coherent Askaryan radio emission from UHE neutrino interactions in the ice, with the goal of detecting the cosmogenic neutrino flux with reasonable event rates. Operating in coincidence with the IceCube neutrino detector would allow complete calorimetry of a subset of the events. We also report on the status of a testbed IceRay station which incorporates both ANITA and IceCube technology and will provide year-round monitoring of the radio environment at the South Pole.

Key words: neutrino detection, Askaryan effect, radio frequency
PACS: 14.60Lm, 95.55.Vj, 98.70.Sa, 84.40.-x

1. Introduction

Continued progress in the determination of the ultra-high energy cosmic ray (UHECR) spectrum above 10^{17} eV has established the presence of the Greisen-Zatsepin-Kuzmin (GZK) suppression [1], resulting from the interaction of UHECRs with the cosmic microwave background (see Fig. 1). Such interactions lead to a "guaranteed" flux of UHE neutrinos, although the characteristics of the flux depend on the details of the source distribution, UHECR composition, and other currently unknown factors. Measurement of the GZK neutrino flux would not only shed light on these issues, but also could indicate the UHECR sources themselves via the direction of the individual neutrinos.

An array to detect UHE neutrinos via their coherent radio emission in a dense medium was originally described by Gusev and Zhelezhykh [2], based on theoretical work by Askaryan. Since then, significant experimental work by the RICE collaboration [3] has established many of the fundamental characteristics of radio transmission in the polar ice, and the ANITA balloon experiment [4] has currently set the best limits on UHE neutrino fluxes. Direct observation of coherent radio emission using an ice target

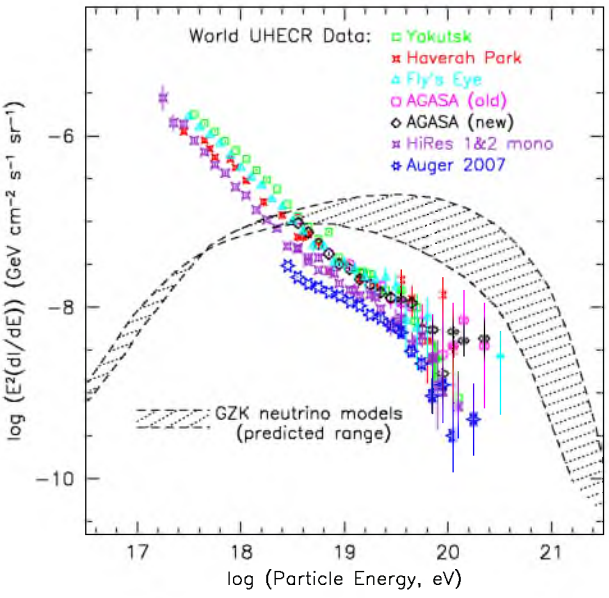

Figure 1: World ultra-high energy cosmic ray and predicted cosmogenic neutrino spectrum as of early 2007, including data from the Yakutsk [5], Haverah Park [6], the Fly's Eye [7], AGASA [8], HiRes [1], and Auger [9], collaborations. Data points represent differential flux $dI(E)/dE$, multiplied by E^2. Error bars are statistical only. GZK neutrino models are from Protheroe & Johnson [10] and Kalashev *et al.* [11].

*Presenter.
Email address: jkelley@icecube.wisc.edu (J. Kelley)

at SLAC has also confirmed the theoretical foundations described by Askaryan [12].

The expected flux of GZK neutrinos is nevertheless quite small, requiring a large array (or in the case of ANITA, a huge target) to ensure reasonable event rates. We propose to extend the IceCube neutrino detector [13] to energies from 10^{17} to 10^{20} eV with a sparse array of radio antennas (IceRay). An initial array of 50 km^2 is designed to provide event rates of O(few/yr) and establish the baseline flux level, while a final target array of 300 to 1000 km^2 could provide $O(100)$ events per year. Centering the array around IceCube allows a subset of the events to be detected in coincidence, providing complete calorimetry of both the initial interaction (via the radio emission) and the outgoing lepton (via the optical emission). While rare, such events provide a valuable means of cross-calibration and reduction of systematics in the absolute energy scale.

2. Design Considerations

We discuss several of the design considerations for a large-scale radio array in the ice, in particular the operating frequency and geometry.

2.1. Operating Frequency

We are initially bounded in operating frequency to the region between several MHz, where backgrounds may be prohibitively large, to around 1 GHz, where the ice becomes opaque. The coherent emission from an Askaryan pulse has a peak field strength which rises linearly with frequency, but the received voltage at an antenna is inversely proportional to frequency, so the direct dependence on frequency cancels when considering the signal-to-noise ratio (SNR). However, a dependence on the bandwidth remains; specifically, we find

$$\mathrm{SNR} \propto E_{\mathrm{shower}} \sqrt{\frac{G\Delta f}{kT_{\mathrm{sys}}Z_0}} \qquad (1)$$

for a shower of energy E_{shower}, using a receiver with gain G and noise temperature T_{sys}, and where Z_0 is a reference impedance. Therefore, high bandwidth is important, but there is no direct dependence on the center frequency of the band.

Other considerations, however, indicate a preference for lower frequencies. First, while the peak field strength of the Čerenkov emission rises with frequency, the angular width of the Čerenkov cone gets narrower [14]. Effectively, this reduces the total solid angle available for detection at high frequencies.

Furthermore, the frequency dependence of the attenuation length of the ice itself plays an important role. Over the 200-700 MHz range, the attenuation length decreases by approximately 25-30% [15]. Because the effective volume, to first order, varies as L^3_{atten}, this implies a strong loss at high frequencies. The overall conclusion is that a high bandwidth, low frequency approach is optimal. Given that a bandwidth factor of 5 is reasonably achievable, we set a preliminary target frequency range of 60-300 MHz.

2.2. Geometry

Because the radio field attenuation length in ice is of O(1 km) [15], one can cover a relatively large area somewhat sparsely. While deploying detectors on the surface is the most cost effective, refraction effects greatly penalize the volumetric acceptance. The index of refraction varies from 1.79 in the deep ice (below about 200m) to 1.33 in the packed snow at the surface [3]. The low-density region is known as the *firn*, and upward-going rays moving through this region are bent away from the surface. This creates a horizon angle — that is, shallower rays cannot reach the detector. This angle gets much less severe as one moves deeper into the ice (see Fig. 2), suggesting that deploying antennas in holes, say, 50m or 200m below the surface is much more efficient.

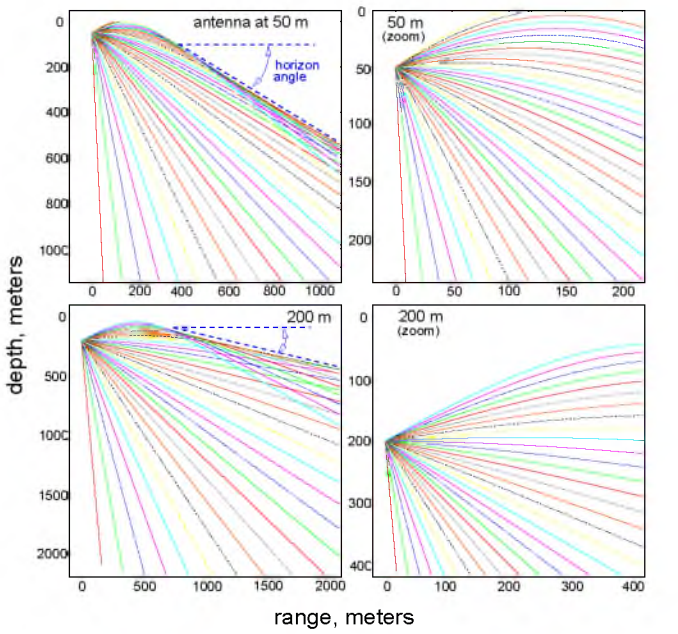

Figure 2: Example of refraction effects for shallower antenna locations. Both 50 m (upper) and 200 m (lower) deep antenna locations are shown. On the left are the wide-scale ray geometries, showing the terminal horizon angle in each case, and on the right the details of the ray bending in the near zone are shown.

IceCube has already developed drilling technology that can be utilized for IceRay. While the enhanced hot water drill (EHWD) used for drilling the 2.5 km deep holes for IceCube string deployment is not mobile enough for our purposes, the independent firn drill (IFD) which drills the "pilot" holes for the EHWD can be easily moved. The IFD is a "hotpoint"-style drill which melts into the firn using a cone of closed-loop copper tubing, heated with a propylene glycol/water mixture. The IFD currently can drill at about 4 m/hour, with an average power usage of

approximately 100 kW. The IFD is effective to depths of 40-50 m, after which pooling water causes power usage to spike. Adding a pump to extract this water is a simple modification which could alleviate this issue. Ultimately, we expect that drilling to 200 m is logistically manageable and cost effective, either with a modified IFD or other technology.

2.3. Baseline Configurations

Given the above design considerations, we focus on two geometries for the initial 50 km^2 phase of the array: a shallower, denser array deployed at a depth of 50 m and with 36 stations; and a deeper, more sparse array deployed at a depth of 200m and with 18 stations. The configurations are chosen to have approximately the same cost and volumetric acceptance in the peak energy region of the GZK neutrino flux, around 10^{18} eV. Figure 3 shows the station arrangement in more detail. Each station consists of three holes separated by 5-10 m, with four antennas (two of each polarization, horizontal and vertical) in each hole. Directionality is achieved for even single-station events via timing information from these local baselines.

3. Simulated Event Rates

The primary IceRay simulation chain is based on Monte Carlo code developed for ANITA and SalSA [16], but independent crosschecks have been performed with ARIANNA [17] and RICE simulation chains. The volumetric acceptance of different array configurations is shown in Fig. 4, and we note reasonable agreement in the important energy range of 10^{18} eV. In general, the 18-station deep configuration gives higher acceptance than the 36-station shallow configuration at the higher energies, but drops off at low energies due to the increased station spacing.

Table 1 shows integrated event rates for the two baselines configuration studied. "Standard" fluxes, such as ESS with a ΛCDM cosmology [18] and Protheroe [**?**], result in approximately 3-10 events per year, but as mentioned earlier, this could vary almost an order of magnitude in either direction depending upon UHECR composition and source evolution. Iron UHECR models in particular tend to produce significantly lower rates [19], although these are currently disfavored by measurements of the spectral endpoint [1]. An important point is that no irreducible backgrounds are expected, so detection of even a few events would be significant.

One significant motivation to build IceRay at the South Pole is to allow for the possibility of coincident, or "hybrid" events with the IceCube detector. A ν_μ or ν_τ event can produce both an initial shower and a long-ranged charged lepton with the potential for detection in both radio and optical channels. A typical geometry for such a hybrid event is shown in Fig. 5.

Such a hybrid event allows cross-calibration of the energy scale of either detector, and while such events are rare, they are background-free. Event rates per ten years for various GZK flux models are shown in table 2. Adding a high energy "guard ring" of strings to IceCube (the "IceCube-plus" configuration; see Ref. [20]) increases the hybrid event rate by up to a factor of two. We have also conservatively assumed here that each detector triggers independently; adding sub-threshold cross-triggering would also increase the event rate.

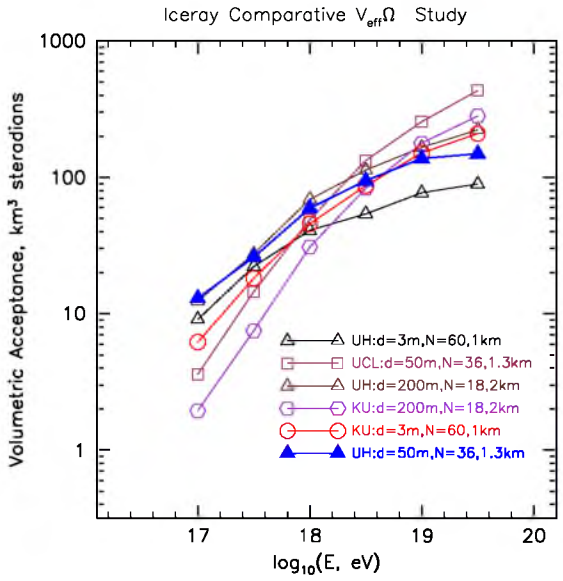

Figure 4: Volumetric acceptance, in km^3 steradian, of various array configurations (d = station depth; N = number of stations; and station spacing), including results from three independent simulation chains.

Table 1: Event rates per year for several classes of UHE cosmogenic neutrino models. The "36-50" rates are for the 36-station, 50m-deep configuration, and the "18-200" rates are for the 18-station, 200m-deep configuration.

Cosmogenic neutrino model	36-50 ev/yr	18-200 ev/yr
Fe UHECR, std. evolution	0.50	0.60
Fe UHECR strong src. evol.	1.6	1.8
ESS 2001,$\Omega_m = 0.3$, $\Omega_\Lambda = 0.7$	3.5	4.4
Waxman-Bahcall-based GZK-ν flux	4.2	4.8
Protheroe and other std. models	4.2-7.8	5.5-9.1
Strong-source evolution (ESS,others)	12-21	13.8-28
Maximal, saturate all bounds	24-40	32-47

4. Testbed Station

Recent data from the ANITA flights have demonstrated that the South Pole is not a particularly radio-quiet environment (at least in the austral summer), but no capability currently exists for year-round monitoring of the natural and anthropogenic backgrounds. To understand and char-

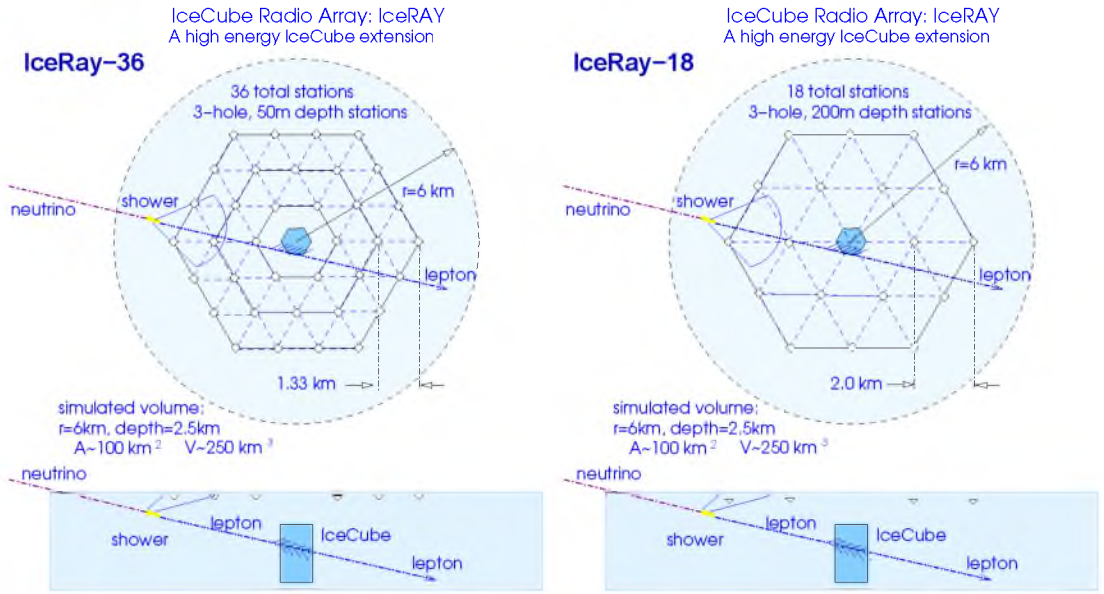

Figure 3: Left: Baseline 36-station, 50 m depth array, in a plan view (top) and side view (bottom) showing the simulated interaction region around the detector. Right: Alternative 200 m depth, 18-station array.

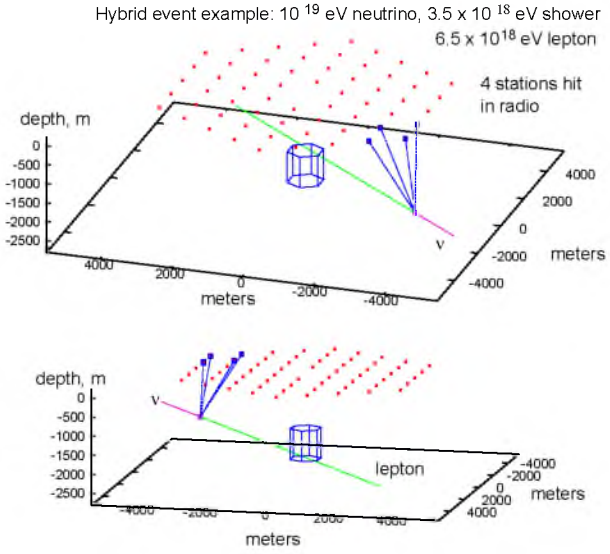

Figure 5: Example of a hybrid event where the vertex is seen by four surface radio detectors and the resulting lepton passes near enough to IceCube to make a detection.

acterize these backgrounds, as well as to test prototype hardware, we have built the IceRay testbed station.

When deployed, the testbed will be a single surface station with pairs of antennas buried in shallow boreholes

Table 2: Hybrid event rates for the baseline IceCube, and IceCube-plus (1.5 km guard ring), per 10 years of operation, for several classes of UHE cosmogenic neutrino models, assuming the IceRay-36, 50m-deep radio array.

Cosmogenic neutrino model	IceCube 10 yrs	IceCube+ 10 yrs
ESS 2001$\Omega_m = 0.3$, $\Omega_\Lambda = 0.7$	3.2	6.4
Waxman-Bahcall-based GZK-ν flux	3.8	7.6
Protheroe and other standard models	3.8-7.1	5.0-8.2
Strong-source evolution (ESS,others)	10-19	13-25
Maximal fluxes, saturate all bounds	22-36	30-44

(2.5 m deep) in the snow. The boreholes are arranged in a circle of radius 5 m. Each hole contains a *discone* antenna optimized for vertically polarized signals, and a *batwing* antenna for horizontally polarized signals. Figure 6 shows the layout of the station as well as the antenna geometry.

The data acquisition system (DAQ) combines hardware elements of ANITA, IceCube, and the digital radio modules of AURA (Askaryan Under-ice Radio Array; see Ref. [22]). Four antennas (two of each polarization) are first fed into a low-noise amplifier chain (with a total gain of $\sim$ 76 dB) in a shielded housing. The combined system has a bandpass of 115 MHz-1.2 GHz. High- and low-frequency components are split and separately digitized with LABRADOR3 ASICs [21] at 2 GSa/s and 1 GSa/s, respectively, as part of the IceCube Radio Readout board (ICRR). The digitized waveforms are buffered and transferred through an intermediary board, the TRACR,

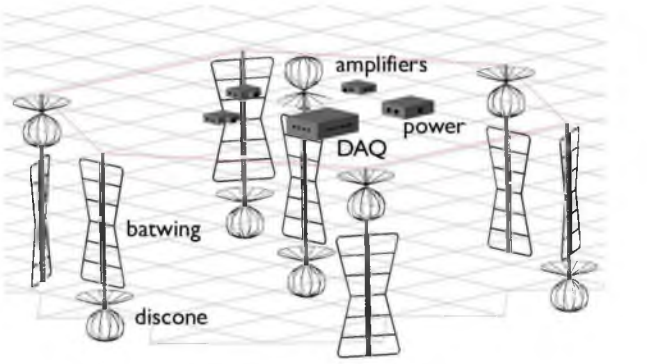

Figure 6: Layout of the IceRay testbed station.

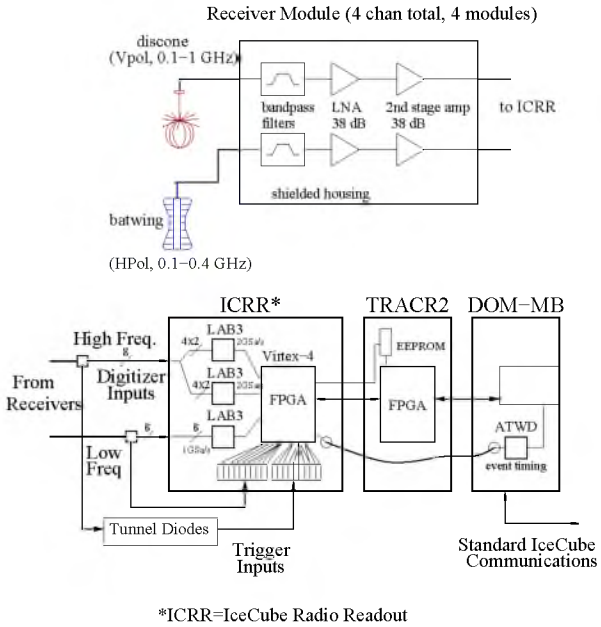

Figure 7: Schematic representation of the data acquisition system for the IceRay testbed station.

to a standard IceCube digital optical module mainboard (DOM-MB), which also provides event time-stamping via its own digitizer, the ATWD. The DOM-MB communicates via the standard IceCube communications protocol, so the station can be connected to the IceCube cabling network and controlled from the IceCube counting house. Furthermore, standard IceCube time calibration procedures can synchronize the DAQ to a GPS clock. Figure 7 shows a schematic of the DAQ components.

5. Outlook

We continue to study open issues with the design of the full array (of order 1000 km^2), such as power distribution and communications. We are also actively pursuing efforts to increase the sensitivity of the system down to the cosmogenic kT noise floor of about -114 dBm/MHz, as well as working with South Pole station management to control the anthropogenic noise in the 60-1000 MHz frequency range, in order to lower our energy threshold below 10^{17} eV. This would both increase the total event rate and provide enhanced opportunities for hybrid events. Furthermore, other techniques such as acoustic detection of UHE neutrinos are developing rapidly, suggesting that a hybrid radio-optical-acoustic array may have significant benefits for systematics and cost [23].

Installation of the IceRay testbed in the austral summer of 2009 will allow precise characterization of the noise environment and will facilitate further development of the 50 km^2 array. IceCube construction will complete in 2011, and we hope to phase in construction of IceRay at that time, as the ability to use IceCube as the core of a GZK neutrino detector is an unparalleled opportunity.

References

[1] R. U. Abbasi *et al.*, Phys. Rev. Lett. **100**, 101101 (2008).
[2] G. A. Gusev and I. M. Zheleznykh, JETP Lett. **38** 10, 611 (1983).
[3] I. Kravchenko *et al.*, Astropart. Phys. **20**, 195 (2003).
[4] S. W. Barwick *et al.*, Phys. Rev. Lett. **96**, 171101 (2006); see also Proc. of Neutrino 2008.
[5] A. V. Glushkov *et al.*, Astropart. Phys. **4**, 15 (1995).
[6] M. A. Lawrence, R. J. O. Reid, and A. A. Watson, J. Phys. G **17**, 733 (1991).
[7] D. J. Bird *et al.*, Astrophys. J. **441**, 144 (1995); J. W. Elbert and P. Sommers, Astrophys. J. **441**, 151 (1995); R. M. Baltrusaitas *et al.*, Phys. Rev. D **31**, 2192 (1985).
[8] S. Yoshida *et al.*, Astropart. Phys. **3**, 105 (1995); S Yoshida and H. Dai, J. Phys. G **24**, 905 (1998).
[9] M. Roth *et al.*, Proc. of 30th ICRC, Mérida, 2007, arXiv:0706.2096.
[10] R. J. Protheroe and P. A. Johnson, Astropart. Phys. **4**, 253 (1996).
[11] O. E. Kalashev, V. A. Kuzmin, D. V. Semikoz and G. Sigl, Phys. Rev. D **66**, 063004 (2002).
[12] P. W. Gorham *et al.*, arXiv:hep-ex/0611008.
[13] M. Ackermann *et al.*, Nucl. Inst. and Meth. **A556**, 169 (2006).
[14] N. Lehtinen, P. Gorham, A. Jacobson, and R. Roussel-Dupré, Phys. Rev. D **69**, 013008 (2004); arXiv:astro-ph/030965.
[15] S. Barwick, D. Besson, P. Gorham, and D. Saltzberg, J. Glaciol. **51**, 231 (2005).
[16] P. W. Gorham *et al.*, Phys. Rev. D **72**, 023002 (2005).
[17] S. W. Barwick, arXiv:astro-ph/0610631.
[18] R. Engel, D. Seckel, and T. Stanev, Phys. Rev. D **64**, 093010 (2001).
[19] M. Ave *et al.*, Astropart. Phys. **23**, 19 (2005).
[20] F. Halzen and D. Hooper, JCAP **0401**, 002 (2004); arXiv:astro-ph/0310152.
[21] G. Varner *et al.*, Nucl. Inst. and Meth. A **583**, 447 (2007).
[22] H. Landsman *et al.*, Proceedings of ARENA 2008, arXiv:0811.2520.
[23] D. Besson *et al.*, Proceedings of ARENA 2008, arXiv:0811.2100.